ORIGINAL ARTICLE

Nose-to-brain delivery of lamotrigine-loaded PLGA nanoparticles

Kuldeep Nigam[1] · Atinderpal Kaur[1] · Amit Tyagi[2] · Md Nematullah[3] · Farah Khan[3] · Reema Gabrani[1] · Shweta Dang[1]

Abstract

Direct nose-to-brain delivery of drugs and faster onset of action have made intra-nasal route a much sought-after alternative to conventional routes of drug delivery to the brain. Lamotrigine is used for the treatment and management of neuropathic pain, and in the present work, lamotrigine (LTG)-PLGA nanoparticles were developed for intra-nasal delivery. The LTG-PLGA nanoparticles were prepared using modified nanoprecipitation method via high-speed homogenization and ultra-sonication techniques. Entrapment efficiency (EE%) of developed LTG-PLGA-NPs was found to be $84.87 \pm 1.2\%$ with drug loading of $10.21 \pm 0.89\%$. The particle size of developed nanoparticles was found to be 184.6 nm with PDI value of 0.082 and zeta potential of -18.8 mV. Dissolution profiles were studied in PBS (pH 7.4), simulated nasal fluid, and simulated cerebrospinal fluid where almost complete release was observed within 5 h in CSF. In vitro, cytotoxicity was analyzed using MTT assay where dose-dependent cytotoxicity was observed for developed LTG-PLGA-NPs. In vitro cytokine analysis showed positive effects of LTG-PLGA-NPs as pro-inflammatory cytokine suppressors. Further, in vivo studies were performed for radiolabeled formulation and drug (^{99m}Tc-LTG-PLGA-NPs and ^{99m}Tc-LTG-aqueous) using Sprague Dawley rats where with the help of gamma scintigraphy studies, various routes of administration viz. oral, intra-nasal, and intra-venous were compared. Various pharmacokinetic parameters were evaluated using biodistribution studies to estimate the drug levels in blood and brain. For ^{99m}Tc-LTG-PLGA-NPs via intra-nasal route, drug targeting efficiency (DTE%) was found to be 129.81% and drug target organ transport (DTP%) to be 22.81% in brain with C_{max} of 3.82%/g within T_{max} 1.5 h. Thus, the developed PLGA nanoparticles for intra-nasal delivery provide a possible alternative for existing available drug formulation for neuropathic pain management.

Keywords Biodistribution · Gamma scintigraphy · Lamotrigine · Nanoparticles · PLGA

Abbreviations

AEDs	Antiepileptic drugs
IL	Interleukin
I.N	Intra-nasal
I.V.	Intra-venous
LTG	Lamotrigine
PLGA	(Poly(lactic-co-glycolic acid)
NPs	Nanoparticles
DTE	Drug target efficiency
DTP	Drug transport percentage
TNF-α	Tumor necrosis factor alpha
IFN-γ	Interferon gamma
^{99m}Tc	Technetium-99m

✉ Shweta Dang
  shweta.dang@jiit.ac.in

1   Department of Biotechnology, Jaypee Institute of Information Technology, A-10, Sector-62, Noida 201309, India

2   Institute of Nuclear Medicine and Allied Sciences, Defence Research and Development Organisation, Timarpur, Delhi 110054, India

3   Department of Biochemistry, Faculty of Science, Jamia Hamdard, New Delhi 110062, India

Introduction

Neuropathic pain is very commonly reported in clinical pharmacology. It is initiated with certain diseases, lesions, or dysfunction in the somatosensory nervous system. Despite the advancement in understanding the etiology of neuropathic pain, its proper management remains a challenge. Neuropathic pain is often associated with multiple clinical conditions such as any chronic or postsurgical nerve injury [1, 2], patients undergoing chemotherapy [3], patients suffering with AIDS [4], and diabetic neuropathy [2].

880

Drug Deliv. and Transl. Res. (2019) 9:879–890

Antiepileptic drugs or commonly known as AEDs are widely reported for the management of pain as they share a common pathophysiology for neuropathy and epilepsy and they help in diminishing neuronal excitability [5, 6]. Lamotrigine (LTG), FDA-approved AED, is widely reported for the first-line management of neuropathic pain, trigeminal neuralgia, etc. because of its ability to block voltage-dependent Na^+ ion channels, thus maintaining the neuronal membrane potential and inhibiting the release of excitatory neurotransmitters such as glutamate [7]. Lamotrigine has high absolute bioavailability of around 98% with maximum plasma concentration (C_{max}) occurs from 1.4 to 4.8 h [8]. Metabolism of lamotrigine is primarily via glucuronic acid conjugation and is eliminated mainly via renal excretion (around 94%). Despite being lipophilic in nature and having high absolute bioavailability, high levels are not retained in the brain, thus challenging its effective analgesic effects along with subcutaneous allergic skin rashes [9]. In addition, LTG shows non-selective distribution profiles upon oral administration, with high levels reaching to non-target organs leading to repetitive dosages and increased number of side effects. Thus, nose to brain delivery can provide the direct delivery to the brain region [10, 11].

Intra-nasal route provides an alternative for the drug delivery to the brain by bypassing the BBB (blood–brain barrier) in a non-invasive mode. Once instilled into the nasal cavity, the drug can reach directly to brain regions via olfactory pathway. The faster onset of action, existence of direct nose-to-brain pathway, and its non-invasive nature make nasal route an attractive route for drug delivery to the brain [12]. However, owing to anatomical features and small volume of nasal cavity, high amount of doses cannot be given through this route; also, drug permeability (especially hydrophilic drugs) is an issue, leading to low bioavailability in brain regions. Nanocarrier-based approach is reported to enhance the permeability of drugs through nasal route and provides a feasible approach for the nose-to-brain pathway [13]. Drugs encapsulated in PLGA nanoparticles are reported to have a controlled release as the polymer encapsulates the drug and forms a matrix [14]. Lamotrigine being a lipophilic drug enters and leaves the brain quickly necessitating the need of a formulation, which could encapsulate the drug and provide for prolonged stay of the drug, once it enters in the brain region.

In the present work, lamotrigine-encapsulated PLGA nanoparticles were developed for nose-to-brain delivery. The LTG-PLGA-NPs were prepared by modified nanoprecipitation method and characterized for particle size, polydispersity index, and zeta potential. Further, in vitro drug release profiles were evaluated in phosphate buffer saline (pH 7.4), simulated nasal fluid (SNF), and simulated cerebrospinal fluid (CSF). LTG-PLGA-NPs were evaluated for cytotoxicity on Neuro-2a cells and modulation of various pro-inflammatory (TNF-α, IFN-γ, and IL-6) and anti-inflammatory cytokines (IL-4 and IL-10) on RAW macrophage cell lines before in vivo experiments. Lamotrigine was radiolabeled with 99^mTc ($99^mTechnetium$ pertechnetate) for evaluating the nose-to-brain pathway. Gamma scintigraphy studies were performed for radiolabeled drug and the corresponding nanoparticles on Sprague Dawley rats. Biodistribution studies were carried out to assess the levels of radiolabeled drug in brain and blood.

Materials and methods

Materials

Lamotrigine was obtained as a generous gift from SNA Healthcare Pvt. Ltd., Mumbai, India. Poly(D,L-lactide-co-glycolide) (PLGA lactide:glycolide (50:50), mol. wt. 30,000–60,000), Poloxamer 407, DMEM, and fetal bovine serum (FBS) were purchased from Sigma-Aldrich (St. Louis, USA). Acetone, dichloromethane, and other organic solvents were purchased from Fisher Scientific (Mumbai, India) and were of HPLC grade. $99^mTechnetium$ pertechnetate was acquired from Regional Centre for Radiopharmaceuticals of the Board of Radiation and Isotope Technology (BRIT), DRDO, Delhi, India. ITLC silica plates were obtained from Gelman Science Inc. (Ann Arbor, MI).

Preparation of lamotrigine-loaded PLGA nanoparticles

Lamotrigine (LTG)-loaded PLGA nanoparticles (LTG-PLGA-NPs) were prepared using nanoprecipitation method slightly modified as in Lalani et al. (2015). Initial solubility studies were carried out for choosing acetone as organic phase for solubility of drug and polymer. Briefly, 5 mg of LTG (based upon initial solubility studies and dose requirement of LTG) and 50 mg of PLGA were dissolved in 2 ml of acetone (drug/polymer ratio of 1:10). The dissolved drug-organic phase was added dropwise (0.5–1 ml/min) with the help of a syringe to 10 ml of 1% (w/v) Poloxamer 407 solution (as aqueous phase) on a magnetic stirrer at 800 rpm. The prepared nanoparticle dispersion was further homogenized using high-pressure homogenizer (tissue master 125 homogenizer, Omni International, Georgia) at 10,000 rpm for 10 min. Further, homogenized nanosuspension was sonicated using probe ultra-sonicator (Model UP400S, Hielscher, Ultrasound Technology, Germany) with an amplitude of 40% for 150 s with 10–10 s on–off cycle. The prepared uniformly homogenized nanoparticles were centrifuged (Centrifuge 5424 R, Eppendorf, Germany) using refrigerated centrifuge at 10,000 rpm, 4 °C, 10 min, and the obtained LTG-PLGA-NP pellet was washed twice to remove any unentrapped drug molecules. The obtained pellet was resuspended in HPLC water for further analysis [15–17].

UV method development and RP-HPLC analysis of lamotrigine

Spectrophotometric detection of lamotrigine was done using double beam spectrophotometer (Shimadzu UV-visible, UV-1800) along with UV-Probe software. Briefly, 10 mg of lamotrigine drug was weighed and dissolved in 10 ml methanol (HPLC grade) and was ultra-sonicated using ultrasonic water bath for 20 min. On complete dissolution of drug in methanol, volume makeup up to 100 ml was done using distilled water in volumetric flask and filtered using Whatman filter paper no. 41. For calibration curve preparation, various dilutions were made and absorbance was taken at 307 nm [18].

For RP-HPLC method development, isocratic system (Waters, Vienna, Austria) was used. Separation was obtained on non-polar SunFire C-18 column (250×4.6 mm, 5 μm). Mobile phase was acetonitrile:monobasic potassium phosphate pH 3.5 (35:65 v/v) and filtered using 0.22-μm syringe filter, ultra-sonicated, and flow rate was maintained at 1.5 ml/min. Twenty microliters of sample was injected and chromatographic peak separations were obtained using UV–Vis detector at 210 nm and peaks were visualized using Breeze Software (Waters, Austria). Calibration curve was plotted by dissolving lamotrigine drug in mobile phase on various dilutions [19].

Encapsulation efficiency and drug loading

The developed LTG-PLGA-NPs were centrifuged at 12,000 rpm as sated above. The supernatant was collected in different vials, and the amount of unentrapped or free drug was calculated by determining the amount of lamotrigine drug using UV spectrophotometer. The encapsulation efficiency and drug loading were calculated using the following equations [20]:

$$Encapsulation\ efficiency\ (EE\%) \tag{1}$$
$$= \left\{ \frac{(total\ amount\ of\ drug - amount\ of\ unentrapped\ drug)}{total\ amount\ of\ drug} \right\}$$
$$\times 100$$

$$Drug\ loading\ (\%) \tag{2}$$
$$= \left\{ \frac{(total\ amount\ of\ drug - amount\ of\ unentrapped\ drug)}{total\ weight\ of\ LTG - PLGA - NPs} \right\}$$
$$\times 100$$

Particle size and zeta potential

The prepared LTG-PLGA-NPs were evaluated for their particle size, polydispersity index, and zeta potential using dynamic scattering spectrometer (Malvern Zetasizer, Malvern Instruments, Worcestershire, UK). Scattering angle was kept at 90° for intensity autocorrelation at 25 °C. The prepared nanoparticles were filtered using 0.22-μm filter membrane and diluted in the ratio of 1:50 using HPLC water, and observations were recorded. For determining the homogeneity in the prepared nanoparticles, PDI values were recorded while for surface charge determination, their zeta potential was recorded [21].

In vitro permeation studies

For preparation of a suitable formulation, it is necessary to study the release profiles of the prepared nanoparticles. In vitro release profiles were carried out using USP type II apparatus (Veego, Mumbai, India) with the help of dialysis membrane (cutoff 12,000 Da, Sigma-Aldrich, St. Louis, USA). Samples were loaded in pre-treated dialysis bags sealed at both ends, and their release profiles were studied in various simulated media (PBS pH 7.4), simulated nasal fluid (pH 5.5), and simulated CSF. Bags were immersed in 200 ml of media at 100 rpm, 37 °C, and periodic samples were aliquoted for detection of released drug quantified with the help of prepared calibration curves. The same amount of fresh media was replaced in the dissolution vessel to maintain the sink conditions [22, 23].

In vitro cytotoxicity studies

The prepared LTG-PLGA-NPs were studied for their toxicity on mammalian cells. Neuro-2a (neuroblastoma cell line, ATCC CCL-131) was used and MTT assay was performed. Neuro-2a cells are brain-derived neuroblastoma cells, and since our formulation and experiments involved neuropathic pain and brain targeting, this cell line was chosen. Cells were grown in Dulbecco's modified Eagle media supplemented with 10% fetal bovine serum with 100 μg/ml penicillin, 100 μg/ml streptomycin, and 2 mmol/l L-glutamine and maintained at 37 °C with 5% CO_2. 1×10^4 cells were seeded in a 96-well plate overnight to acclimatize on the surface. Different concentrations of prepared LTG-PLGA-NPs, placebo-NPs, and aqueous LTG drug were added and treatment was done for 18 h. MTT dye was added thereafter while formazan crystals were dissolved in DMSO and absorbance was recorded at 570 nm using scanning multiwall spectrophotometer [24]. The cytotoxicity was evaluated by calculating percentage viability using the following equation:

$$\%\text{cell viability} = \frac{Absorbance\ of\ treated\ cells}{Absorbance\ of\ untreated\ cells} \times 100 \tag{3}$$

In vitro cytokine analysis

The RAW murine macrophage cell lines were cultured in DMEM supplemented with 10% FBS and penicillin (100 U/ml) and streptomycin (100 μg/ml) and maintained at 37 °C with

882

Drug Deliv. and Transl. Res. (2019) 9:879–890

5% CO_2 in a humidified incubator. The RAW cells were plated into 24-well plates for all experiments. After reaching subconfluency, cells were treated with LPS (100 ng/ml) for 6 h. The cells were then treated with different drugs at a concentration of 50 μg/ml for 24 h. After 24-h incubation, supernatant was collected from each treatment group, centrifuged at 2000×g for 10 min at 4 °C, and supernatant was collected. All cytokines (TNF-α, IFN-γ, IL-4, IL-6, and IL-10) were measured using mouse ELISA kits of Krishgen Biosystems (Mumbai, India). Briefly, ELISA plates were coated with standard and sample supernatant of different treatment groups (100 μl/well), sealed and incubated according to manufacturer's instructions. The wells were washed four times with wash buffer, and each well was incubated with the detection antibody for 2 h and then again washed four times and incubated with streptavidin-HRP for 1 h at room temperature. Each well was incubated with tetramethylbenzidine (TMB) substrate solution for 30 min at room temperature, and then, the reaction was stopped with stop solution. The results were read using a microplate spectrophotometer at 450 nm within 30 min of stopping reaction. A standard curve prepared from cytokines was used to calculate the cytokine production of the samples [25].

Radiolabeling of LTG and LTG-PLGA-NPs

For radiolabeling experiments, [99m]-Technicium pertechnetate (^{99m}Tc) was used. A known amount of drug was dissolved in aqueous-based solution along with reducing agent such as stannous chloride (2 mg/ml) along with [99m]Tc (200 μl, 5 mCi). The mixture was then incubated for 30 min at room temperature. The concentration of $SnCl_2$ and incubation time were optimized for drug tagging which was evaluated with the help of silica-coated thin-layer chromatography (Gelman Sciences, Inc., Ann Arbor, MI, USA) with acetone as mobile phase [26]. The drug tagging and stability were then performed on rat blood plasma to validate the radiolabeling efficiency [27]. Radiolabeling efficiency was estimated with the help of the following equation [28]:

$$\%Radiolabelling\ efficiency$$
$$= \frac{Radioactive\ counts\ attained\ in\ lower\ half\ of\ strip}{Total\ radioactive\ counts\ in\ the\ strip} \times 100 \tag{4}$$

Gamma scintigraphy

All the in vivo experiments were done at the Institute of Nuclear and Applied Medicine, DRDO, Delhi, with prior ethical clearance obtained from IAEC (IAEC, New Delhi, IAEC vide number INM/IAEC/16/10), and proper guidelines were followed. For animal studies, Sprague Dawley rats (3–

4 months old, ~200 g) were taken. Ketamine hydrochloride (50 mg/ml) was used as an anesthetizing agent delivered via intra-peritoneal injection. Rats were divided into five groups consisting of three animals for each time point (0.5, 1.5, 3, 6, and 24 h). Three groups consisted of radiolabeled nanoparticle formulation (^{99m}Tc-LTG-PLGA-NPs) delivered via oral, intra-nasal, and intra-venous routes, and in other two groups, radiolabeled lamotrigine aqueous (^{99m}Tc-LTG) was delivered via intra-nasal and I.V. routes. Thin catheter (diameter 0.1 mm) was used to deliver the radiolabeled formulation intra-nasally. Single photon emission CT gamma camera (SPECT, LC 75-005, Siemens, Germany) was used to take the periodic images at different time points to get an overview on distribution profile of radiolabeled drug [26].

Biodistribution studies

Biodistribution studies were carried out to check the amount of radiolabeled drug that was actually reaching blood and brain. Sprague Dawley rats (3–4 months old, 180–200 g) were taken for the study and divided into four groups consisting of three animals per groups for each time points (0.5, 1.5, 3, 6, and 24 h). For anesthetizing, ketamine hydrochloride (50 mg/ml) was given via intra-peritoneal injection. Radiolabeled nanoparticle formulation (^{99m}Tc-LTG-PLGA-NPs) delivered via intra-nasal and intra-venous routes and radiolabeled lamotrigine aqueous (^{99m}Tc-LTG) via intravenously and blood was drawn by puncturing retro-orbital vein. The brain was dissected out by sacrificing the rat via spinal dislocation method, washed in normal saline, and weighed. The amount of radioactivity present in the organ was determined using a shielded well-type gamma camera, and various pharmacokinetic parameters such as radioactivity per gram of tissue, drug target efficiency (DTE%), and drug transport percentage (DTP%) were evaluated using the following equations [26, 29, 30]:

$$\%Radioactivity/g\ of\ tissue$$
$$= \frac{Counts\ in\ sample \times 100}{wt.\ of\ sample \times total\ counts\ injected} \tag{5}$$

$$Drug\ targeting\ efficiency\ (DTE\%)$$
$$= \left[\frac{\left(\frac{AUC\ brain}{AUC\ blood}\right)I.N.}{\left(\frac{AUC\ brain}{AUC\ blood}\right)I.V.} \right] \times 100 \tag{6}$$

$$Drug\ transport\ percentage\ (DTP\%)$$
$$= 90\% \frac{(Bi.n.-Bx)}{Bi.n.} \times 100 \tag{7}$$

$$Bx = \frac{Bi.v.}{Pi.v.} \times Pi.n. \tag{8}$$

where

Bx   AUC of brain contributed by systemic circulation via intra-venous administration

Bi.v. $AUC_{(0-24)}$ of brain via intra-venous administration

Pi.v. $AUC_{(0-24\ h)}$ of blood via intra-venous administration

Bi.n. $AUC_{(0-24\ h)}$ of brain via intra-nasal administration

Pi.n. $AUC_{(0-24\ h)}$ of blood via intra-nasal administration

Statistical analysis

Results obtained were analyzed using GraphPad Prism (Ver. 05). ANOVA analysis (one-way) was applied on various results and p value ≤ 0.05 was taken as statistically significant.

Results

Entrapment efficiency, size, PDI, and zeta potential

For estimation of lamotrigine, UV spectra were run and standard plot was plotted and 307 nm was observed as λ_{max}. Similarly, RP-HPLC calibration curve was plotted using acetonitrile:monobasic potassium phosphate (35:65 v/v) as mobile phase. The developed LTG-PLGA-NPs were centrifuged and supernatant was taken to estimate the amount of unentrapped lamotrigine. 1:10 ratio (drug:polymer) was found suitable in our experiments giving high entrapment efficiency. Ratios lower than 1:10 showed poor entrapment efficiency (< 70%). The entrapment efficiency percentage was calculated and it was found to be $84.87 \pm 1.2\%$. The nanoparticle pellet was weighed after washing thrice with distilled water, and drug loading (%) was calculated to be $10.21 \pm 0.89\%$. These values were validated using RP-HPLC. Further, the particles were characterized for particle size which were found to be of nanometric range of 184.6 nm, PDI value of 0.082, and zeta potential of $- 18.8$ mV (Fig. S1 and Fig. S2).
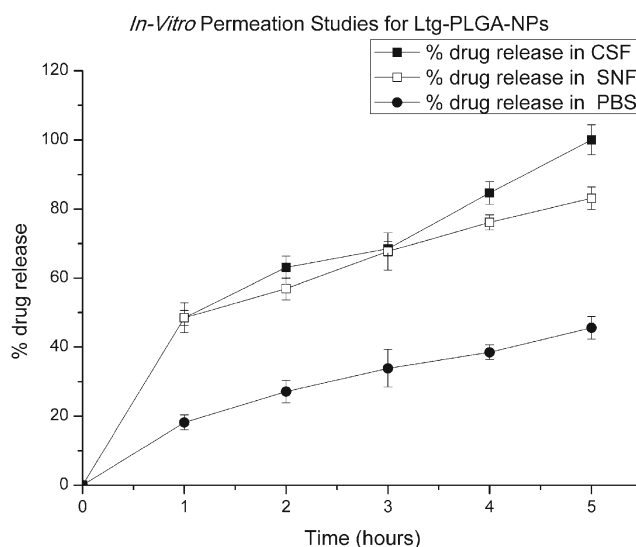
In vitro permeation studies

It was observed that around 60% of release was obtained in CSF and SNF within 2 h, which reached to 100% in CSF within 5 h while being around 83% in SNF, which reached to 100% within 24 h. However, the release was comparably slow in PBS (pH 7.4), around 33% in the first 3 h which reached to around 75% in 24 h (Fig. 1). Further, dissolution profiles were evaluated by fitting them into various kinetic models. Based on their R^2 values, it was observed that the LTG-PLGA-NPs followed zero-order release ($R^2 = 0.9797$) and Korsmeyer–Peppas model ($R^2 = 0.9541$) in CSF [31].

In vitro cytotoxicity and cytokine analysis

In vitro toxicity was evaluated for LTG-NPs, LTG Aq. drug, and placebo NPs for the concentration range from 0.625 to 50 µg/ml covering the reported C_{max} value of 1.7 µg/ml [8]. Dose-dependent cytotoxicity was observed in the prepared formulation where LTG-PLGA-NPs showed higher cell viability as compared with Aq. drug. LTG-PLGA-NPs showed around 86–98% cell viability for concentrations of 2.5−0.625 µg/ml whereas corresponding Aq. drug showed comparatively higher level of cytotoxicity among N2-a cells with around 79–90% cell viability only (Fig. 2).

In vitro cytokine analysis showed that the lamotrigine-loaded PLGA nanoparticles showed high potential in suppressing the levels of pro-inflammatory cytokines (TNF-α, IL-6, and IFN-γ) as compared with its aqueous counterparts. The levels of TNF-α for LTG-PLGA-NPs were found to be 551.83 ± 19.46 pg/ml compared with 585.49 ± 15.7 pg/ml for LTG-aqueous (Fig. 3a). These levels were just borderline higher than prepared nanoparticles. Similarly, for IL-4, the levels were found to be 314.19 ± 5.3 pg/ml and 668.1 ± 7.15 pg/ml for LTG-PLGA-NPs and LTG-Aq. respectively (Fig. 3b). For IL-6, levels were seen as 101.71 ± 1.09 pg/ml for LTG-PLGA-NPs and 157.71 ± 4.96 pg/ml (Fig. 3c). However, the levels of IL-10 were almost the same for both LTG-PLGA-NPs (105.65 ± 1.99 pg/ml) and LTG-Aq. (109.61 ± 3.96 pg/ml) (Fig. 3d). On the contrary, significant variation was observed in the levels of IFN-γ ranging from 129.4 ± 13.8 pg/ml in LTG-PLGA-NPs to 444.51 ± 12.6 pg/ml in LTG-Aq. (Fig. 3e) (with p value < 0.05).

Fig. 1 In vitro permeation studies in simulated cerebrospinal fluid (CSF), simulated nasal fluid (SNF), and phosphate buffer saline (PBS, pH 7.4). Results are represented as mean ± S.E.M. for each group

884

Drug Deliv. and Transl. Res. (2019) 9:879–890

Fig. 2 In vitro cytotoxicity analysis on Neuro-2a cell lines via MTT assay (% cell viability of prepared LTG-PLGA-NPs, LTG-Aq., and corresponding placebo NPs). Results are represented as mean ± S.E.M. for each group with *p* values < 0.05
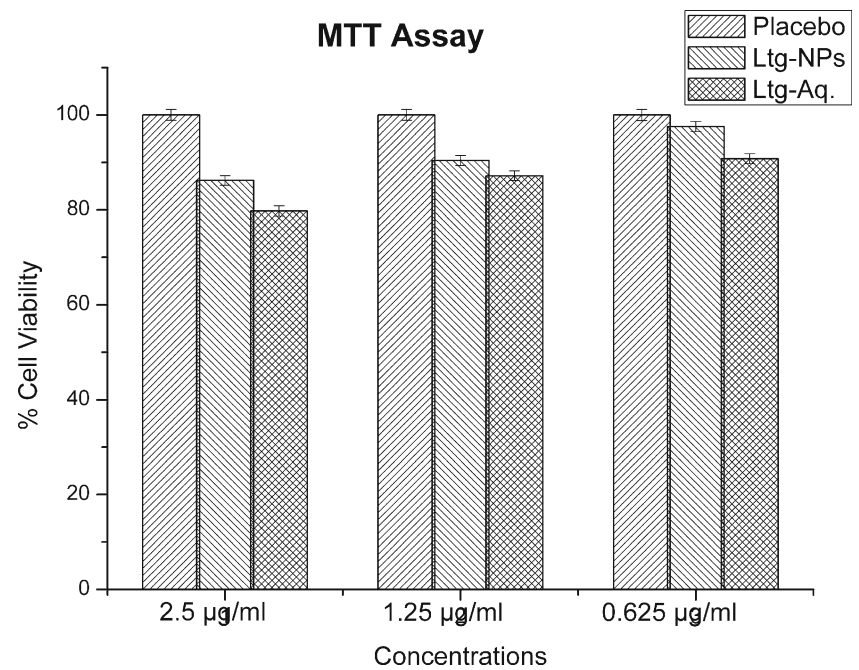

In vivo pharmacokinetics experiments

The radiolabeling efficiency of the drug was determined with the help of ITLC method and was found to be 97.08 ± 1.1%. Further, the stability of radiolabeled drug was determined in normal saline and blood serum for 24 h and was found to be 95 ± 0.9% similar to that observed earlier. The stable radiolabeling suggested using formulation with radiolabelled drug to perform further scintigraphy and biodistribution studies.
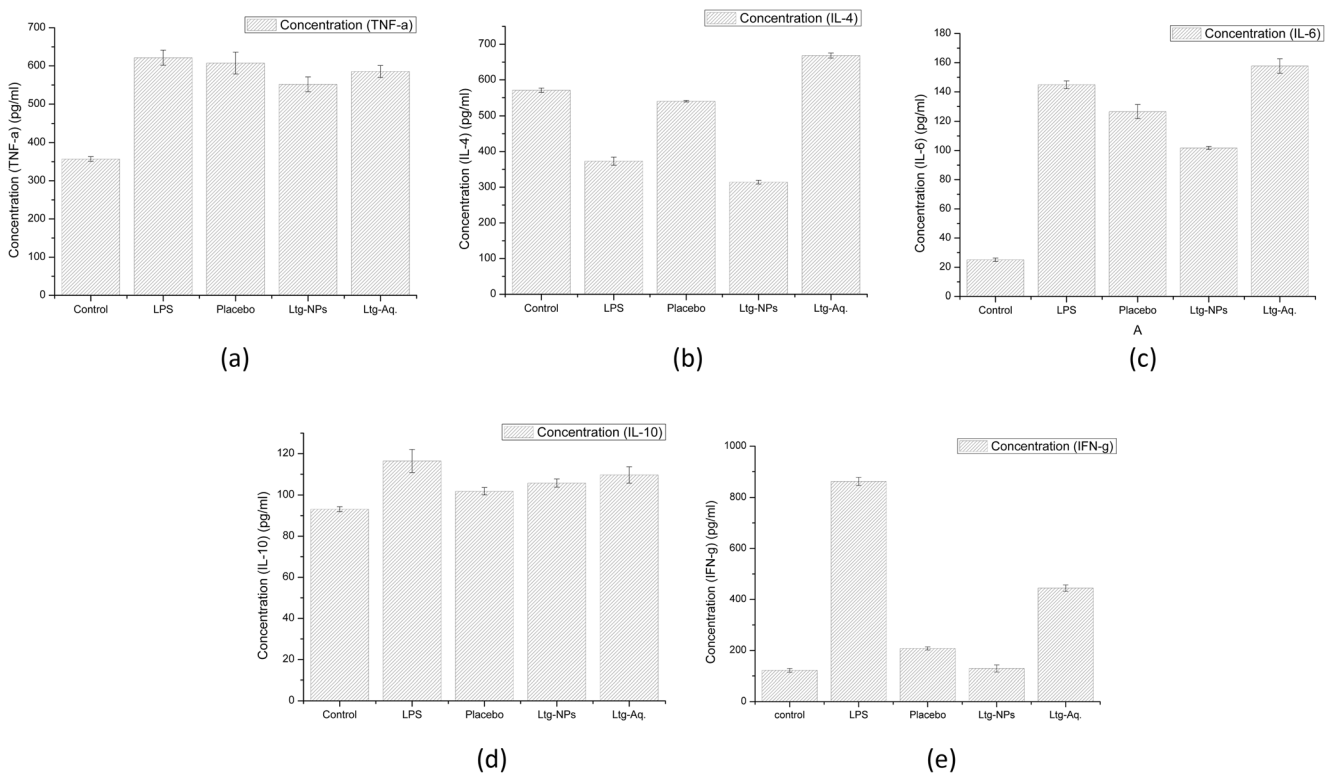
Fig. 3 Cytokine levels by untreated RAW macrophages (control), after bacterial lipopolysaccharide treatment, placebo group, LTG-NPs, and Aq. lamotrigine for **a** tumor necrosis factor alpha (TNF-α), **b** interleukin-4 (IL-4), **c** interleukin-6 (IL-6), **d** interleukin-10 (IL-10), and **e** interferon-γ (IFN-γ). Results are represented as mean ± S.E.M. for each group with *p* values < 0.05
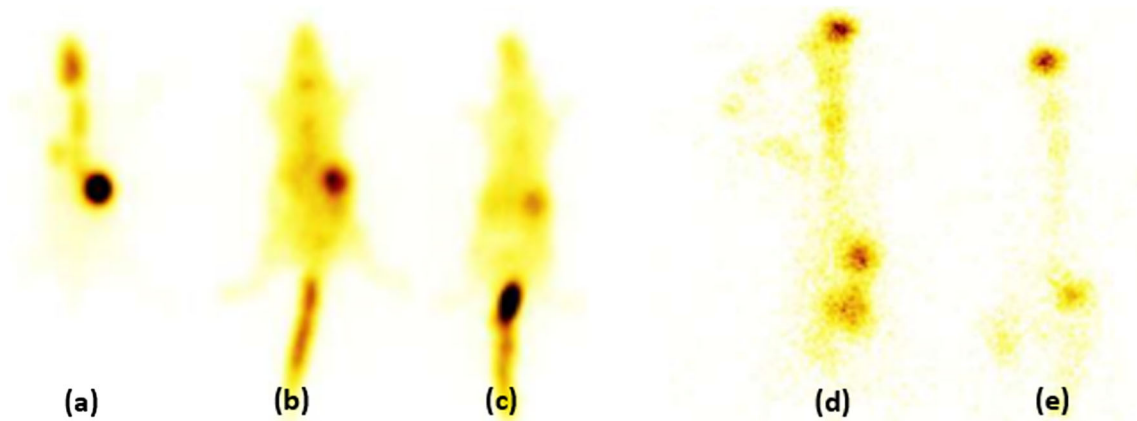
Fig. 4 Gamma scintigraphy image of **a** oral ^{99m}Tc-LTG-PLGA-NPs, **b** I.V. ^{99m}Tc-LTG-aqueous, **c** I.V. ^{99m}Tc-LTG-PLGA-NPs, **d** I.N. ^{99m}Tc-LTG-aqueous, and **e** I.N. ^{99m}Tc-LTG-PLGA-NPs showing presence of radioactivity in different organs after 0.5 h

It was observed from gamma scintigraphy studies that major accumulation of ^{99m}Tc-LTG-PLGA-NPs was in abdominal organs when administered orally as seen in Figs. 4a and 5a while very small amount reaching to the actual target organ, i.e., brain, in 0.5 h and 1.5 h. Rapid distribution of ^{99m}Tc-LTG-PLGA-NPs was seen via I.V route from 0.5 h (Fig. 4c) to 1.5 h (Fig. 5c) which was comparatively higher than that of ^{99m}Tc-LTG-Aq. for the same time points (Figs. 4b and 5b).

Upon intra-nasal administration of ^{99m}Tc-LTG-PLGA-NPs and ^{99m}Tc-LTG-Aq., it was seen that ^{99m}Tc-LTG-Aq. were distributed to various peripheral organs including stomach area (Figs. 4d and 5d) while ^{99m}Tc-LTG-PLGA-NPs were retained near the brain region in higher amounts with less distribution to other peripheral organs as compared with its aqueous counterparts (Figs. 4e and 5e) [9].

With biodistribution studies, it was observed that on intra-nasal administration, significantly higher value of C_{max} of 3.82%/g was achieved at T_{max} 1.5 h for ^{99m}Tc-LTG-PLGA-NPs in brain samples (Fig. 6) as compared with C_{max} value of 2.06%/g for ^{99m}Tc-LTG-aqueous as same T_{max} (Tables 1 and 2). In addition, it was observed upon I.V. administration,

^{99m}Tc-LTG-PLGA-NPs were able to achieve significantly higher value of C_{max} 3.55%/g in blood (Fig. 7) and 2.73%/g in brain which were quite high as compared with ^{99m}Tc-LTG-aqueous 2.89%/g in blood while 1.4%/g in brain at T_{max} (1.5 h). Further, pharmacokinetic parameters, drug targeting efficiency (DTP%), and drug target organ transport (DTP%) were evaluated. For ^{99m}Tc-LTG-PLGA-NPs upon intra-nasal route, DTE% of 129.81% and DTP% of 22.96% were observed (Table 3).

Discussion

Lamotrigine-loaded PLGA nanoparticles were successfully developed using modified nanoprecipitation method with high EE%. High drug loading percentage suggested higher amount of drug loaded in the nanoparticles [32, 33]. Nanoparticles were characterized for particle size, which were found to be of nanometric range of 184.6 nm. The polydispersity index was obtained to be of 0.082 which suggested a high level of uniformity and homogeneity among the particles. Zeta
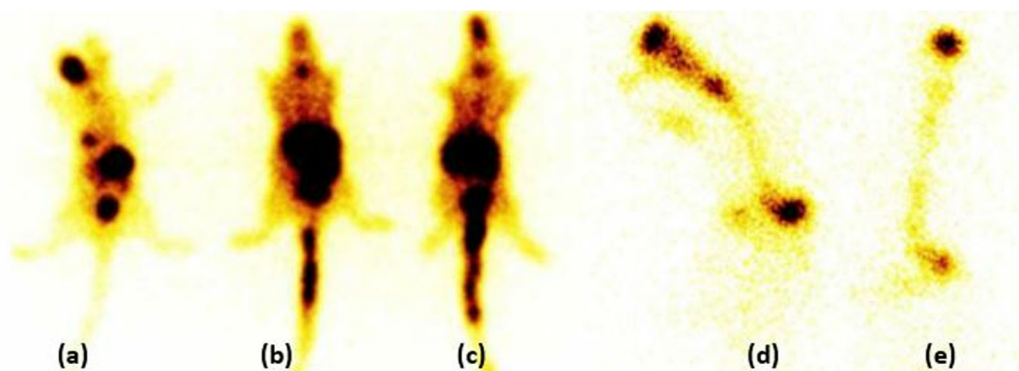
Fig. 5 Gamma scintigraphy image of **a** oral ^{99m}Tc-LTG-PLGA-NPs, **b** I.V. ^{99m}Tc-LTG-aqueous, **c** I.V. ^{99m}Tc-LTG-PLGA-NPs, **d** I.N. ^{99m}Tc-LTG-aqueous, and **e** I.N. ^{99m}Tc-LTG-PLGA-NPs showing presence of radioactivity in different organs after 1.5 h

886

Drug Deliv. and Transl. Res. (2019) 9:879–890

Fig. 6 Drug concentration in brain samples of rat showing ^{99m}Tc-LTG-PLGA-NPs and ^{99m}Tc-LTG-aqueous (intra-venous and intra-nasal)
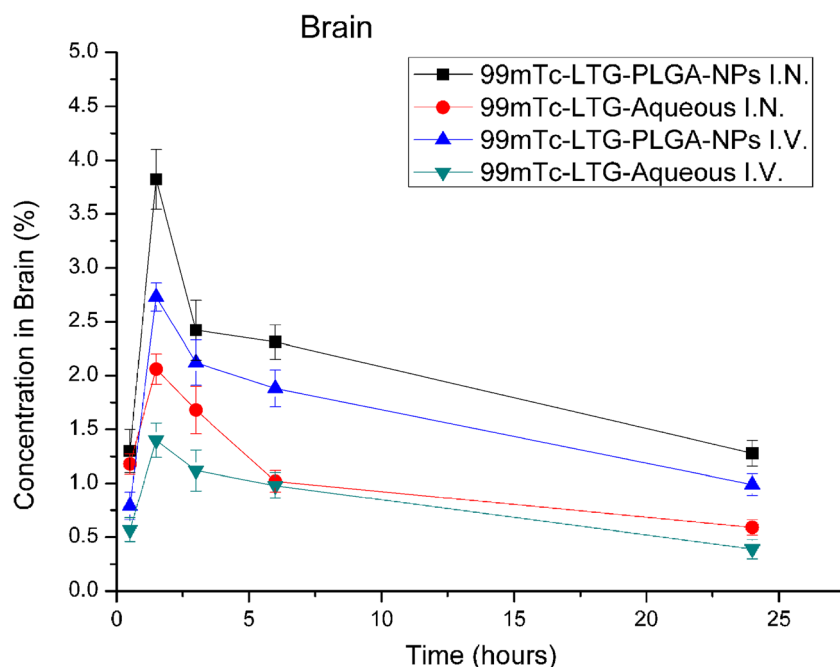
potential was obtained to be − 18.8 mV which could be due to the negative charge imparted because of PLGA (which carries negative charge because of the presence of terminal carboxylic group) [17] and the surfactant Poloxamer 407 belongs to non-ionic class. One of the problems associated with intranasal delivery is poor permeation of drug across nasal mucosa resulting in low concentration of drug reaching to the brain. The lamotrigine-encapsulated PLGA nanoparticles could penetrate the nasal mucosa and can be transported to the brain in effective concentration owing to their small size [34].

In vitro permeation studies were carried out using dialysis membrane in various simulated media where around 60% release was observed in the first 2 h in SNF and CSF; this release can be attributed to drug being adsorbed on the surface of PLGA nanoparticles. The permeation data was fitted into various release models and it was found to follow Korsmeyer–

Peppas model suggesting an initial swelling of polymeric matrix followed by gradual release of lamotrigine drug from the swollen matrix [35, 36]. The release component ("n" value = 0.4273) suggested Fickian diffusion pattern where the flow of lamotrigine drug through the dialysis membrane is directly proportional to the concentration gradient. With time, the concentration of lamotrigine attains equilibrium by releasing out from the swollen polymeric matrix [37].

In vitro cell line–based experiment showed higher percentage cell viability for drug nanoparticles as compared with aqueous drug formulation even at very high concentration ranges. Also, corresponding placebo nanoparticles showed highest cell viability percentage suggesting PLGA as a suitable nanocarrier for lamotrigine nanoparticles. These results were found to be significant with one-way ANOVA analysis with $p < 0.05$.

Table 1 Distribution of ^{99}Tc-LTG-PLGA-NPs and ^{99}Tc-LTG-aqueous (intra-nasal and intra-venous) in Sprague Dawley rats in percentage per gram

Formulation and route of administration	Distribution of lamotrigine (NPs and aqueous) at different sampling time points					
	Organ	0.5 h	1.5 h	3 h	6 h	24 h
^{99m}Tc-LTG-PLGA-NPs I.N.	Blood	0.5 ± 0.1	0.87 ± 0.13	1.86 ± 0.19	2.69 ± 0.14	0.95 ± 0.09
^{99m}Tc-LTG-PLGA-NPs I.N.	Brain	1.3 ± 0.2	2.42 ± 0.28	3.82* ± 0.28	2.31 ± 0.16	1.28 ± 0.12
^{99m}Tc-LTG-aqueous I.N.	Blood	0.26 ± 0.17	1.04 ± 0.18	1.86 ± 0.11	1.18 ± 0.2	0.82 ± 0.08
^{99m}Tc-LTG-aqueous I.N.	Brain	1.18 ± 0.094	2.06 ± 0.14	1.68 ± 0.22	1.02 ± 0.1	0.59 ± 0.07
^{99m}Tc-LTG-PLGA-NPs I.V.	Blood	1.66 ± 0.22	3.55* ± 0.18	2.96 ± 0.23	1.99 ± 0.19	1.04 ± 0.09
^{99m}Tc-LTG-PLGA-NPs I.V.	Brain	0.79 ± 0.08	1.88 ± 0.13	2.73 ± 0.21	2.12 ± 0.17	0.99 ± 0.1
^{99m}Tc-LTG-aqueous I.V.	Blood	1.46 ± 0.18	2.89 ± 0.21	2.02 ± 0.13	1.28 ± 0.17	0.99 ± 0.11
^{99m}Tc-LTG-aqueous I.V.	Brain	0.57 ± 0.11	1.1 ± 0.16	1.12 ± 0.19	0.98 ± 0.12	0.39 ± 0.09

*Statistically significant outcomes at p value < 0.05 have been reported

Table 2 Pharmacokinetics of ^{99}Tc-LTG-PLGA-NPs and ^{99}Tc-LTG-aqueous (intra-nasal and intra-venous) in Sprague Dawley rats
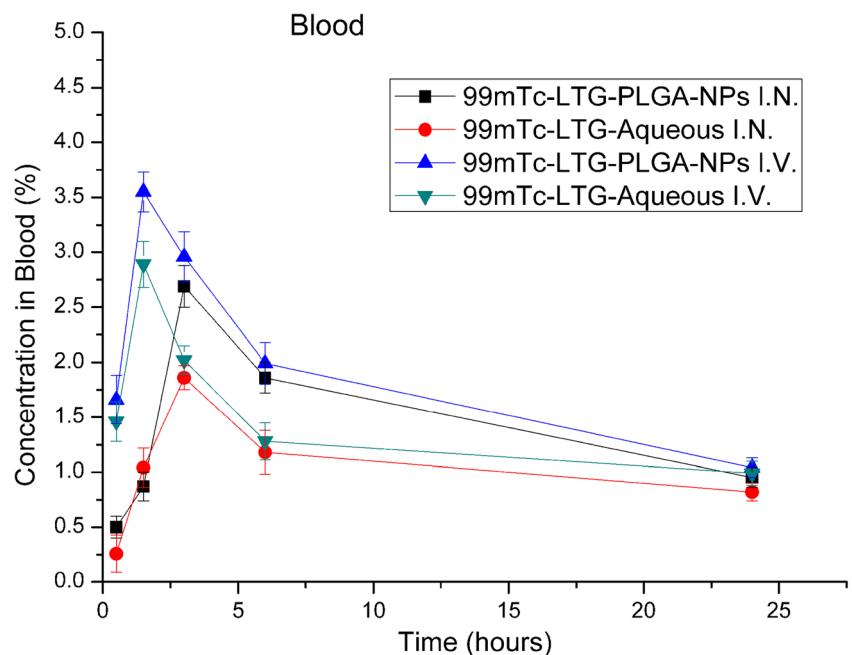
Formulation and route of administration	Organ	C_{max} (%/gm)	T_{max} (h)	AUC$_{0-24\ h}$
^{99m}Tc-LTG-PLGA-NPs I.N.	Blood	2.6	3	35.6
^{99m}Tc-LTG-PLGA-NPs I.N.	Brain	3.82*	1.5	46.97
^{99m}Tc-LTG-aqueous I.N.	Blood	1.86	3	25.45
^{99m}Tc-LTG-aqueous I.N.	Brain	2.06	1.5	23.26
^{99m}Tc-LTG-PLGA-NPs I.V.	Blood	3.55*	1.5	42.6
^{99m}Tc-LTG-PLGA-NPs I.V.	Brain	2.73	1.5	43.3
^{99m}Tc-LTG-aqueous I.V.	Blood	2.89	1.5	31.6
^{99m}Tc-LTG-aqueous I.V.	Brain	1.4	1.5	18.5

*Statistically significant outcomes at p value < 0.05 have been reported

The unregulated inflammatory responses script the progression of various inflammatory diseases. Lipopolysaccharide (LPS) is found in outer part of Gram-negative bacteria, and it is a well-known activator of macrophages and other immune cells [38]. It stimulates the production of various pro-inflammatory cytokines such as IL-6, TNF-α, and IFN-γ in macrophages through TLR pathway [39]. Cytokines are broadly classified as pro-inflammatory and anti-inflammatory cytokines based upon their role in inflammation. Pro-inflammatory cytokines (IL-6, TNF-α, IFN-γ) promote the inflammation process whereas anti-inflammatory cytokines (IL-4, IL-10) are the suppressors of these pro-inflammatory cytokines. For a successful formulation mediating inflammation process, it must be noted that it should decrease the levels of pro-inflammatory cytokines (ones' promoting the inflammation) or/and upregulating the levels of these anti-inflammatory cytokines. The levels of these cytokines were detected using ELISA kits in RAW macrophage cell lines

as per the manufacturer's protocols. LPS (bacterial origin) is an agonist to toll-like receptors (TLR 4) and is widely reported as an activator/inducer of inflammation [40, 41] and hence taken as control for cytokine upregulation.

LPS-induced TNF-α or the "master regulator" of inflammation is a potent activator of macrophages and other immune cells through the activation MAPK pathway, and synergistically with IFN-γ activate NF-$\kappa\beta$ [42]. The levels of TNF-α were borderline low; however, the levels of IFN-γ and IL-6 were comparatively quite low against the aqueous counterparts. It has been widely reported that in various neuropathic conditions, such as rheumatoid arthritis and ankylosing spondylitis [43, 44], the levels of TNF-α and IL-6 are elevated. The significant decrease observed by LTG-PLGA-NPs suggests that it is a potential inflammation suppressor by lowering the production levels of pro-inflammatory cytokines in macrophages (with p value < 0.05). On the contrary, LTG-PLGA-NPs did not show any significant

Fig. 7 Drug concentration in blood samples of rat showing ^{99m}Tc-LTG-PLGA-NPs and ^{99m}Tc-LTG-aqueous (intra-venous and intra-nasal)

Table 3 Drug targeting efficiency and direct target organ transport following intra-nasal administration of ^{99}Tc-LTG-PLGA-NPs

Formulation and route of administration	Target organ	Drug targeting efficiency (DTE%)	Direct target organ transport (DTP%)
^{99}Tc-LTG-PLGA-NPs	Brain	129.81	22.96

effect on anti-inflammatory cytokines. Lamotrigine drug in aqueous form showed higher upregulation of IL-4 as compared with nanoparticles. However, both nanoparticles and Aq. drug did not show significant upregulation of IL-10. These results strongly suggested that potential of existing lamotrigine as immuno-modulator was increased in the form of LTG-PLGA-NPs where it significantly downregulated the level of pro-inflammatory cytokines (IL-6, TNF-α, and IFN-γ) whereas existing drug formulation was able to only upregulate the level of IL-4.

Lamotrigine was radiolabeled with ^{99m}Tc to trace the absorption and distribution of drug to various parts of body. The ^{99m}Tc-LTG-PLGA-NPs were given via oral, intra-nasal, and intra-venous routes. The purpose was to compare the distribution of drug via various routes of administration. In the preliminary gamma scintigraphy studies, it was clearly observed that ^{99m}Tc-LTG-PLGA-NPs when given via intra-nasal route were reaching in higher amount in the brain regions as compared with aqueous drug and were retained in this area. This observation confirmed the transport of lamotrigine via nose-to-brain pathway. However, gamma images of ^{99m}Tc-LTG-PLGA-NPs given via oral route showed lesser drug in the brain region, and higher drug retention was observed in the GI tract. The Aq. drug when administered intra-nasally reaches buccal cavity, which is a common opening for mouth and nose. The small amount reaching this area is transported to the stomach area through esophagus (similar as food/oral drug administration). Gamma images of ^{99m}Tc-LTG-PLGA-NPs given via intra-venous route also showed higher drug concentrations in systemic pool.

A comparative intra-nasal vs. intra-venous biodistribution study confirmed the patterns observed in gamma scintigraphy studies. Significantly, higher values of drug were found in the brain upon intra-nasal application of ^{99m}Tc-LTG-PLGA-NPs, as compared with those in blood. Upon intra-venous administration of ^{99m}Tc-LTG-PLGA-NPs, it was observed that the drug was in higher concentration in systemic circulation as compared with brain regions, indicating that the drug is not able to cross BBB in desired concentrations [45]. Despite having high bioavailability (~ 98%), the main problem with lamotrigine, being a lipophilic molecule, is the low retention time in the brain [9]. With biodistribution studies, it was clearly seen that lamotrigine-loaded PLGA nanoparticles were able to permeate efficiently and were able to be retained in the brain for longer duration. The brain targeting efficiency of ^{99m}Tc-LTG-PLGA-NPs given via intra-nasal route was compared with intra-venous route by calculating DTE% where it was found to be 129.8% (as compared with intra-venous route taken as 100%). DTE% compares

the delivery of drug to the target organ (brain) following intra-nasal administration vs. intra-venous administration. Higher DTE% shows higher amount of drug accumulated at target site. More than 100% DTE values show higher onsite targeting and accumulation of LTG-PLGA-NPs efficiently in the brain via i.n. route. DTP% measures the relative contribution of direct intra-nasal route in the delivery to the target organ (brain). The obtained DTE% and DTP% were acceptable and showed promising outcomes for nose-to-brain delivery.

Conclusion

Lamotrigine-loaded PLGA nanoparticles were developed via modified nanoprecipitation method using high-pressure homogenizer and ultra-sonication techniques. The developed LTG-PLGA-NPs were characterized for particle size, zeta potential, and PDI and were found to be in nanometric ranges. Dissolution profiles were studied using PBS (pH 7.4), SNF, and CSF to understand their permeation mechanisms. Cytotoxicity was evaluated using MTT assay on neuro-2a cell lines and various cytokine levels in macrophage cell lines. Further, in vivo animal studies were performed in Sprague Dawley rats where gamma scintigraphy studies were performed to assess oral, intra-nasal, and intra-venous routes for LTG-PLGA-NPs which were validated by biodistribution studies. Studies suggested that PLGA is a suitable carrier system for lamotrigine and intra-nasal as suitable route for neuropathic pain management.

Compliance with ethical standards

All institutional and national guidelines for the care and use of laboratory animals were followed.

Conflict of interest The authors declare that there is no conflict of interest.

Drug Deliv. and Transl. Res. (2019) 9:879–890

889

References

1. Siddall PJ, McClelland JM, Rutkowski SB, et al. A longitudinal study of the prevalence and characteristics of pain in the first 5 years following spinal cord injury. Pain. 2003;103(3):249–57.

2. Kehlet H, Jensen TS, Woolf CJ. Persistent postsurgical pain: risk factors and prevention. Lancet. 2006;367(9522):1618–25.

3. Caraceni A, Portenoy RK. An international survey of cancer pain characteristics and syndromes. Pain. 1999;82(3):263–74.

4. Hewitt DJ, McDonald M, Portenoy RK, Rosenfeld B, Passik S, Breitbart W. Pain syndromes and etiologies in ambulatory AIDS patients. Pain. 1997;70(2–3):117–23.

5. McNamara J. Drugs acting on the central nervous system. Goodman and Gilman's the pharmacological basis of therapeutics. 9th ed. New York: McGraw-Hill; 1996. p. 461–86.

6. Han HC, Lee DH, Chung JM. Characteristics of ectopic discharges in a rat neuropathic pain model. PAIN®. 2000;84(2–3):253–61.

7. Chong E, Dupuis LL. Therapeutic drug monitoring of lamotrigine. Ann Pharmacother. 2002;36(5):917–20.

8. Srichaiya A, Longchoopol C, Oo-Puthinan S, Sayasathid J, Sripalakit P, Viyoch J. Bioequivalence of generic lamotrigine 100-mg tablets in healthy Thai male volunteers: a randomized, single-dose, two-period, two-sequence crossover study. Clin Ther. 2008;30(10):1844–51.

9. Castel-Branco M, Lebre V, Falcao A, Figueiredo I, et al. Relationship between plasma and brain levels and the anticonvulsant effect of lamotrigine in rats. Eur J Pharmacol. 2003;482(1–3):163–8.

10. Löscher W, Ganter M, Fassbender CP. Correlation between drug and metabolite concentrations in plasma and anesthetic action of ketamine in swine. Am J Vet Res. 1990;51(3):391–8.

11. Walker MC, Tong X, Perry H, Alavijeh MS, Patsalos PN. Comparison of serum, cerebrospinal fluid and brain extracellular fluid pharmacokinetics of lamotrigine. Br J Pharmacol. 2000;130(2):242–8.

12. Hanson LR, Frey WH. Intranasal delivery bypasses the blood-brain barrier to target therapeutic agents to the central nervous system and treat neurodegenerative disease. BMC Neurosci. 2008;9(3):S5.

13. Chaturvedi M, Kumar M, Pathak K. A review on mucoadhesive polymer used in nasal drug delivery system. J Adv Pharm Technol Res. 2011;2(4):215–22.

14. Gentile P, Chiono V, Carmagnola I, Hatton P. An overview of poly (lactic-co-glycolic) acid (PLGA)-based biomaterials for bone tissue engineering. Int J Mol Sci. 2014;15(3):3640–59.

15. Bilati U, Allémann E, Doelker E. Strategic approaches for overcoming peptide and protein instability within biodegradable nano- and microparticles. Eur J Pharm Biopharm. 2005;59(3):375–88.

16. Sharma D, Maheshwari D, Philip G, Rana R, Bhatia S, Singh M, et al. Formulation and optimization of polymeric nanoparticles for intranasal delivery of lorazepam using Box-Behnken design: in vitro and in vivo evaluation. Biomed Res Int. 2014;2014:1–14.

17. Lalani J, Patil S, Kolate A, et al. Protein-functionalized PLGA nanoparticles of lamotrigine for neuropathic pain management. AapsPharmscitech. 2015;16(2):413–27.

18. Shinde VR, Shelake MR, Shetty SS, Chavan-Patil AB, Pore YV, Late SG. Enhanced solubility and dissolution rate of lamotrigine by inclusion complexation and solid dispersion technique. J Pharm Pharmacol. 2008;60(9):1121–9.

19. Emami J, Ghassami N, Ahmadi F. Development and validation of a new HPLC method for determination of lamotrigine and related compounds in tablet formulations. J Pharm Biomed Anal. 2006;40(4):999–1005.

20. Ranjan AP, Mukerjee A, Helson L, Vishwanatha JK. Scale up, optimization and stability analysis of curcumin C3 complex-loaded nanoparticles for cancer therapy. J Nanobiotechnol. 2012;10(1):38.

21. Romero-Pérez A, García-García E, Zavaleta-Mancera A, Ramírez-Bribiesca JE, Revilla-Vázquez A, Hernández-Calva LM, et al. Designing and evaluation of sodium selenite nanoparticles in vitro to improve selenium absorption in ruminants. Vet Res Commun. 2010;34(1):71–9.

22. Martinac A, Filipović-Grčić J, Perissutti B, Voinovich D, Pavelić Ž. Spray-dried chitosan/ethylcellulose microspheres for nasal drug delivery: swelling study and evaluation of in vitro drug release properties. J Microencapsul. 2005;22(5):549–61.

23. Mohanraj K, Sethuraman S, Krishnan UM. Development of poly (butylene succinate) microspheres for delivery of levodopa in the treatment of Parkinson's disease. J Biomed Mater Res B Appl Biomater. 2013;101(5):840–7.

24. Sharma A, Gupta S, Sarethy IP, Dang S, Gabrani R. Green tea extract: possible mechanism and antibacterial activity on skin pathogens. Food Chem. 2012;135(2):672–5.

25. Sharma Y, Bashir S, Khan MF, et al. Inhibition of Src homology 2 domain containing protein tyrosine phosphatase as the possible mechanism of metformin-assisted amelioration of obesity induced insulin resistance in high fat diet fed C57BL/6J mice. Biochem Biophys Res Commun. 2017;487(1):54–61.

26. Kaur A, Saxena Y, Bansal R, Gupta S, Tyagi A, Sharma RK, et al. Intravaginal delivery of polyphenon 60 and curcumin nanoemulsion gel. AAPS PharmSciTech. 2017;18(6):2188–202.

27. Sharma D, Sharma RK, Sharma N, Gabrani R, Sharma SK, Ali J, et al. Nose-to-brain delivery of PLGA-diazepam nanoparticles. AAPS PharmSciTech. 2015;16(5):1108–21.

28. Rastogi R, Sultana Y, Aqil M, et al. Alginate microspheres of isoniazid for oral sustained drug delivery. Int J Pharm. 2007;334(1–2):71–7.

29. Keck JP, McElroy SL. Clinical pharmacodynamics and pharmacokinetics of antimanic and mood-stabilizing medications. J Clin Psychiatry. 2002;63:3–11.

30. Kumar M, Misra A, Babbar AK, Mishra AK, Mishra P, Pathak K. Intranasal nanoemulsion based brain targeting drug delivery system of risperidone. Int J Pharm. 2008;358(1–2):285–91.

31. Cojocaru V, Ranetti AE, Hinescu LG, et al. Formulation and evaluation of in vitro release kinetics of Na3CaDTPA decorporation agent embedded in microemulsion-based gel formulation for topical delivery. Farmacia. 2015;63(5):656–64.

32. Shen S, Wu Y, Liu Y, Wu D. High drug-loading nanomedicines: progress, current status, and prospects. Int J Nanomedicine. 2017;12:4085–109.

33. Zheng S, Xie Y, Li Y, et al. Development of high drug-loading nanomicelles targeting steroids to the brain. Int J Nanomedicine. 2014;9:55.

34. Dong X. Current strategies for brain drug delivery. Theranostics. 2018;8(6):1481–93.

35. Singhvi G, Singh M. In-vitro drug release characterization models. Int J Pharm Stud Res. 2011;2(1):77–84.

36. Kim DH, Martin DC. Sustained release of dexamethasone from hydrophilic matrices using PLGA nanoparticles for neural drug delivery. Biomaterials. 2006;27(15):3031–7.

37. Fu Y, Kao WJ. Drug release kinetics and transport mechanisms of non-degradable and degradable polymeric delivery systems. Expert Opin Drug Deliv. 2010;7(4):429–44.

38. Mantovani A, Sica A, Sozzani S, et al. The chemokine system in diverse forms of macrophage activation and polarization. Trends Immunol. 2004;25(12):677–86.

39. Hamilton TA. Molecular basis of macrophage activation: from gene expression to phenotypic diversity. Macrophage. 2002;2:73–102.

40. Hines DJ, Choi HB, Hines RM, Phillips AG, MacVicar BA. Prevention of LPS-induced microglia activation, cytokine production and sickness behavior with TLR4 receptor interfering peptides. PLoS One. 2013;8(3):e60388.

41. Murray CL, Skelly DT, Cunningham C. Exacerbation of CNS in-flammation and neurodegeneration by systemic LPS treatment is independent of circulating IL-1β and IL-6. J Neuroinflammation. 2011;8(1):50.

42. Dinarello CA. Proinflammatory cytokines. Chest. 2000;118(2): 503–8.

43. Liu W, Wu YH, Zhang L, et al. Elevated serum levels of IL-6 and IL-17 may associate with the development of ankylosing spondyli-tis. Int J Clin Exp Med. 2015;8(10):17362.

44. Yan Y, Guo TM, Zhu C. Effects of non-steroidal anti-inflammatory drugs on serum proinflammatory cytokines in the treatment of an-kylosing spondylitis. Biochem Cell Biol. 2018;96:450–6.

45. Nigam K, Kaur A, Tyagi A, Manda K, Gabrani R, Dang S. Baclofen-loaded poly (d, l-lactide-co-glycolic acid) nanoparticles for neuropathic pain management: in vitro and in vivo evaluation. Rejuvenation Res 2018. https://doi.org/10.1089/rej.2018.2119.